Trans-Channel Interactions in Batrachotoxin-Modified Skeletal Muscle Sodium Channels: Voltage-Dependent Block by Cytoplasmic Amines, and the Influence of μ-Conotoxin GIIIA Derivatives and Permeant Ions

Evgeny Pavlov, Tatiana Britvina, Jeff R. McArthur, Quanli Ma, Iván Sierralta, Gerald W. Zamponi, and Robert J. French
Department of Physiology and Biophysics, University of Calgary, Calgary, Alberta, Canada

ABSTRACT External μ-conotoxins and internal amine blockers inhibit each other's block of voltage-gated sodium channels. We explore the basis of this interaction by measuring the shifts in voltage-dependence of channel inhibition by internal amines induced by two μ-conotoxin derivatives with different charge distributions and net charges. Charge changes on the toxin were made at residue 13, which is thought to penetrate most deeply into the channel, making it likely to have the strongest individual interaction with an internal charged ligand. When an R13Q or R13E molecule was bound to the channel, the voltage dependence of diethylammonium (DEA)-block shifted toward more depolarized potentials (23 mV for R13Q, and 16 mV for R13E). An electrostatic model of the repulsion between DEA and the toxin simulated these data, with a distance between residue 13 of the μ-conotoxin and the DEA-binding site of ~15 Å. Surprisingly, for tetrapropylammonium, the shifts were only 9 mV for R13Q, and 7 mV for R13E. The smaller shifts associated with R13E, the toxin with a smaller net charge, are generally consistent with an electrostatic interaction. However, the smaller shifts observed for tetrapropylammonium than for DEA suggest that other factors must be involved. Two observations indicate that the coupling of permeant ion occupancy of the channel to blocker binding may contribute to the overall amine-toxin interaction: 1), R13Q binding decreases the apparent affinity of sodium for the conducting pore by ~4-fold; and 2), increasing external [Na^+] decreases block by DEA at constant voltage. Thus, even though a number of studies suggest that sodium channels are occupied by no more than one ion most of the time, measurable coupling occurs between permeant ions and toxin or amine blockers. Such interactions likely determine, in part, the strength of trans-channel, amine-conotoxin interactions.

INTRODUCTION

It has been recognized for more than 30 years that, in general, the degree of block of a membrane channel by an ionic blocker depends on transmembrane voltage. This voltage dependence is generally thought to reflect, at least in part, the electrical work performed as the blocking ion traverses part of the electric field in the channel en route from the solution bathing the membrane to its binding site in the channel's conducting pore (1–3). For example, amine blockers of sodium channels enter from the cytoplasmic side of the channel and block more strongly at positive voltages (4,5). Voltage dependence can be characterized by an effective valence, $z\delta$. Here, z is the charge on the blocker, and δ is the electrical distance, or fraction of the transmembrane voltage that the blocker charge penetrates. The half-inhibition potential, V_h, can be expressed in terms of the blocker's intrinsic binding affinity in the absence of an applied voltage. Thus, shifts in voltage dependence of a block provide a convenient indication of changes in the blocker's binding affinity. We use such shifts to monitor changes in the affinity of cytoplasmically applied amine blockers, when a charged conotoxin derivative binds to the extracellular mouth of a sodium channel.

A similar strategy was used to investigate the interaction between the positively charged voltage sensor of a voltage-gated sodium channel and μ-contoxin derivative, R13Q (6). In that particular case, a simple electrostatic interpretation explained the discrete inhibitory shift in voltage-dependent activation of a single channel caused by the binding of R13Q to the channel. In the same study, preliminary experiments indicated a similar inhibition of channel block by internally applied diethylammonium (DEA). In that analysis, one clue that the inhibitory interactions were electrostatic was that it was essential to account for the partial screening of toxin charges by counterions in the external solution, to simulate the observed shifts.

Data presented by Ma et al. (7) demonstrate that the binding of positively charged μ-conotoxin derivatives (R13Q, nominal net charge, +5; R13E, nominal net charge, +4) decreases the affinity of positively charged amine blockers to the channel, consistent with an electrostatic component in the interaction between the two types of blockers. Residue 13 on the toxin is thought to penetrate most deeply into the pore, and is thus likely to be positioned near the amine-binding site (8–11). Here, we further test this electrostatic hypothesis by measuring the shifts in voltage-dependence of the amine block, caused by the binding of μ-conotoxin derivatives bearing different charges. We model the contribution of the bound toxin to the electrostatic potential inside the channel, and demonstrate that general properties of the experimentally measured interactions are consistent with trans-channel electrostatic repulsion between external and internal blockers. However, the calculations suggest that a precise ac-

Submitted May 23, 2008, and accepted for publication July 9, 2008.

Address reprint requests to Robert J. French, Dept. of Physiology and Biophysics, University of Calgary, 3330 Hospital Drive NW, Calgary, Alberta T2N 4N1, Canada. Tel.: 403-220-6893; Fax: 403-210-7446; E-mail: french@ucalgary.ca.

Editor: Dorothy A. Hanck.

0006-3495/08/11/4277/12 $2.00
doi: 10.1529/biophysj.108.138297

count of some of the more subtle differences between the two amines will require a more elaborate model. Additional experiments provide evidence that toxin-binding modifies the occupancy of the channel by Na^+, and that alteration of the Na^+ gradient modifies the amine block at a constant voltage. Thus, it is likely that the coupling of toxin and amine-binding to a redistribution of permeant ions in the pore partially determines the properties of the trans-channel interaction, even though, on average, the sodium channel is likely to accommodate only a single Na^+ ion in the narrow part of the pore.

MATERIALS AND METHODS

Single-channel recordings and analysis of voltage-dependent block

All materials, protocols, and single-channel analyses used in these experiments were essentially the same as in Ma et al. (7). Analysis of the voltage-dependence of the block of single-channel currents by DEA and tetrapropylammonium (TPrA) followed the simplest version of the Woodhull analysis, by fitting a simple Boltzmann function to plots, against voltage, of either fractional residual current (DEA) or open/unblocked probability (TPrA). Further details are presented in Results (see Fig. 3).

Electrostatic modeling

The potential contribution inside the model channel, created by the binding of a μ-conotoxin molecule to the vestibule, was obtained by solving the following boundary value problem. In regions containing ionic solution, the potential, ϕ, was described by the linearized Poisson-Boltzmann equation:

$$-\nabla^2\varphi + \kappa^2\varphi = 0, \quad (1)$$

where $\kappa = 1/\lambda$, and λ is the Debye length.

In purely dielectric regions, potential was governed by the Laplace equation:

$$-\nabla^2\varphi = 0. \quad (2)$$

Standard boundary conditions were applied. The potential was continuous across dielectric boundaries, and the jump of the normal component of the electric displacement was set equal to $4\pi\sigma$, where σ is the surface-charge density at the boundaries. The charge of μ-conotoxin was considered to be distributed uniformly over its surface. Thus, the toxin charge affected the numerical solution for the potential only through these boundary conditions.

The boundary element method (BEM) was used to solve this boundary value problem. This method has been used mostly for engineering applications in areas such as elasticity, fluid dynamics, and heat transfer (12). In a biophysical context, it was applied in calculations of the electrostatic potential of macromolecules with complicated shapes exposed to a surrounding solution (13,14), and for the calculation of electrostatic forces acting on an ion inside the channel in Brownian dynamics simulations (15,16). The BEM is a powerful approach for systems with complicated geometry, because it is easily adapted to accommodate complex shapes.

All programming and calculations, including the determination of parameters required to fit the theoretical model to experimental data, were performed using Mathematica 4.1 software. Further details are presented below, in conjunction with the results of calculations (see Figs. 5 and 6).

RESULTS

We obtained an experimental measure of the change in binding energy of an amine blocker of a Na channel when a polycationic μ-conotoxin binds at the opposite (extracellular) end of the channel. The change in binding energy is most directly determined as the shift in voltage at which the channel is blocked 50% of the time, which occurs when μ-conotoxin binds. We then asked whether the observed shifts are consistent with an electrostatic model, based on approximate, but realistic, geometric and electrical parameters for the channel.

Voltage-dependence of amine block, and its dependence on μ-conotoxin binding

As demonstrated in Ma et al. (7), μ-conotoxin and amine blockers reduce each other's channel-blocking activity when added from opposite sides of the membrane. Here, we compare the voltage-dependence of channel block by amine blockers of a toxin-free channel with that seen during discrete events when the channel is partially blocked by the μ-conotoxin. Fig. 1 gives examples of current traces recorded in such an experiment, using 24 mM DEA. First, in the control, currents through the channel were recorded at various voltages in the presence of ''extracellular'' R13E, and in the absence of DEA. Then DEA was added to the ''cytoplasmic'' chamber, and currents were recorded at the same voltages as in the control. The DEA block was evaluated separately for toxin-bound and toxin-free states of the channel. The long durations of toxin-bound and unbound times, and their different, easily recognizable current levels, allowed an analysis of toxin-bound and toxin-free states from the same trace. For each

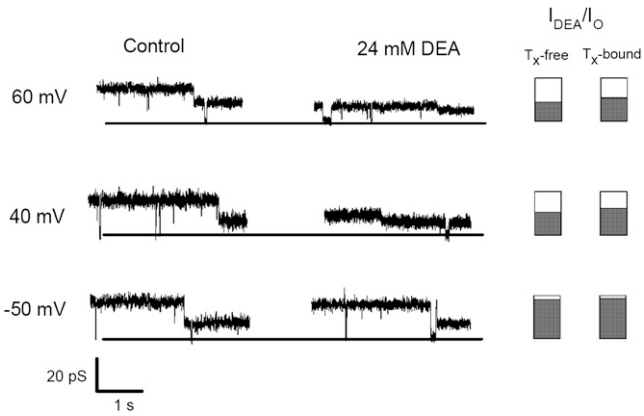

FIGURE 1 Single-channel records show voltage-dependence of fast channel block by DEA of the fully open channel, and of the channel partially blocked by μ-conotoxin mutant R13E. Records were selected to show partially blocked level at right-hand end of each of six traces. Addition of DEA results in fast block, which scales down the current to an increasing degree as the voltage is made more positive. In controls without DEA, but in the presence of R13E, the channel can be found either in the fully open state with a current amplitude of I_O-Tx-free, or partially blocked with current amplitude of I_O-Tx-bound. In the presence of 24 mM DEA, current amplitude is characterized by the toxin-free state, I_{DEA}-Tx-free, and the toxin-bound state, I_{DEA}-Tx-bound. The DEA-unblocked fraction of single-channel current, at different voltages, was calculated as a ratio between current amplitudes in the absence and presence of DEA for the toxin-free and the toxin-bound channel (*solid segments, bar graphs at right*).

voltage, we measured the ratio of current amplitudes in the presence and absence of DEA, as shown in the bar graphs alongside each trace in Fig. 1.

In the case of TPrA, blocking kinetics were slow enough to resolve discrete, all-or-none blocking events, albeit of much shorter mean duration than those resulting from the conotoxin block. Currents were recorded with both μ-conotoxin and TPrA simultaneously present on opposite sides of the membrane (Fig. 2), allowing control data and toxin-bound data to be extracted from a single continuous trace. The probability of channel block by the amine blocker was defined as $(1 - p_O)$, where p_O is the channel ''open'' probability in the presence of TPrA. In the range of voltages used, $p_O \approx 1$ in the absence of TPrA. Open probabilities, indicated in the bar graphs at the right hand end of each trace in Fig. 2, were determined from the mean open and blocked times obtained from dwell-time histograms (see Ma et al. (7)).

Shift in voltage-dependence of channel block by amines, caused by trans-channel interaction with μ-conotoxin derivatives

Experimental data, collected as described above, were used for estimation of the voltage shift caused by μ-conotoxin binding. To this end, the probabilities that the channel was not blocked by amine, with and without the μ-contoxin derivative bound, were plotted as a function of voltage for four different types of experiments: DEA-R13E (Fig. 3 *A*), DEA-R13Q (Fig. 3 *B*), TPrA-R13E (Fig. 3 *D*), and TPrA-R13Q (Fig. 3 *E*). Each data point was obtained by averaging values obtained from 3–8 separate single-channel experiments. Plots were fit

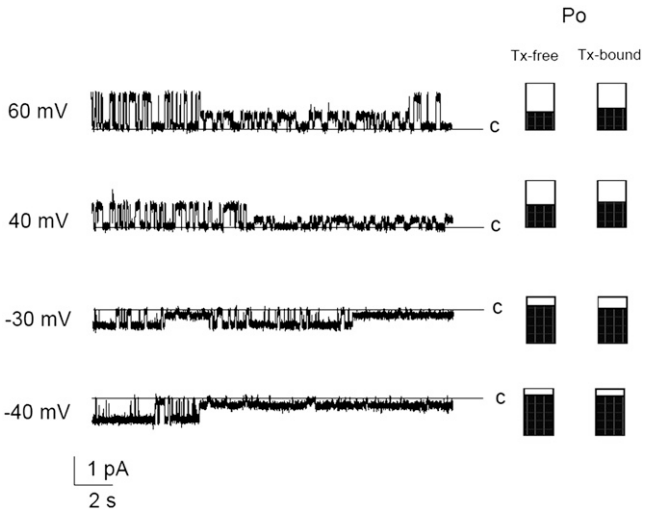

FIGURE 2 Single-channel records show voltage-dependence of channel block by TPrA of fully open channel, and of the channel partially blocked by μ-conotoxin mutant R13Q. In this experiment, R13Q was added to the chamber facing the outer vestibule of the channel, with 5 mM TPrA present in the opposite chamber. The degree of channel block, $(1 - p_O)$, by TPrA of open or toxin-bound channels was determined from mean open and blocked times obtained from dwell-time histograms (*open segments, bar graphs at right*). Solid segments in bar graphs represent p_O.

by Boltzmann functions to determine the midpoint voltage, where the block by amine is 50% (V_h), and the apparent valence ($z\delta$). Fitting parameters V_h and $z\delta$ are presented in Fig. 3, *C* and *F*, and Table 1. Voltage shifts were estimated as differences between values of V_h obtained under different conditions.

The binding of R13Q or R13E caused positive shifts in the voltage-dependence of the DEA block, without systematically or substantially changing the slope (proportional to $z\delta$). The fact that $z\delta$ did not change significantly implies that toxin-binding did not cause any detectable change in the DEA-binding site. The shift caused by R13Q binding is 23 ± 2 mV (the error estimate indicated for the shift is the sum of mean $\pm$ SE values for the individual V_h estimates), and that caused by R13E binding is 16.0 ± 1.8 mV. The greater shift caused by R13Q (nominal net charge, +5) than by R13E (nominal net charge, +4) is qualitatively consistent with an electrostatic interaction between μ-conotoxin and DEA. A model is presented below, to describe the potential distribution arising from the presence of the μ-conotoxin in the channel's vestibule.

It is interesting that the voltage shifts of the TPrA block, associated with R13Q and R13E binding, appear to be systematically smaller than those for DEA (Table 1). This suggests that DEA and TPrA cannot be quantitatively modeled as point charges binding at exactly the same site in the channel, despite apparent valences for their block that are, for practical purposes, indistinguishable. Nonetheless, the qualitative features of the interactions between the two amines and the conotoxin derivatives, represented by the directions of the shifts, are identical.

In the case of TPrA, for which discrete blocking events can be resolved, both mean open/unblocked and closed/blocked times were voltage-dependent, with closed times increasing (Fig. 4 *A*), and open times decreasing, as voltage increases (Fig. 4 *B*). The magnitudes of slopes were similar, suggesting that TPrA surmounts an energy barrier that is nearly symmetric with respect to the applied electric field when binding to, or dissociating from, its binding site. Thus, association and dissociation reactions contribute approximately equally to the voltage-dependence of a steady-state block. A simplistic interpretation of this voltage-dependence is that TPrA actually occludes the pore at the peak of the energy barrier, partway along the reaction coordinate toward its stable blocking position. However, without a more detailed experimental study, it is not possible to identify unambiguously the physical basis of the voltage-dependence. A more critical examination of some of the general issues is provided in the Discussion.

Calculation of the toxin's contribution to the electrostatic potential inside the channel

As shown above, experimental measurements of voltage-dependence of the channel block allowed us to estimate the electrostatic potential induced by two differently charged

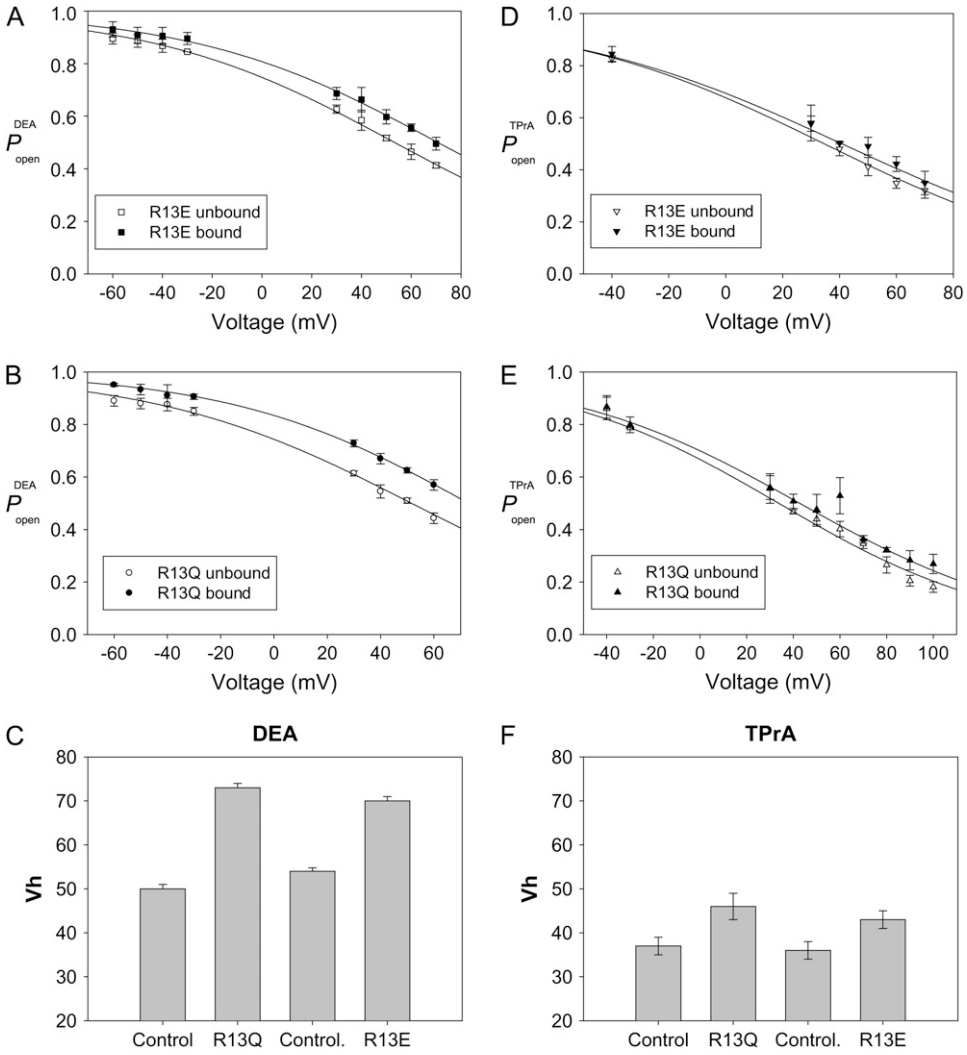

FIGURE 3 Shifts of voltage-dependence of amine block associated with toxin-binding, indicating inhibitory interaction between toxin and amino-blocker. (*A*) R13E-DEA. (*B*) R13Q-DEA. (*C*) Voltages for 50% block, *Vh*, for DEA. (*D*) R13E-TPrA. (*E*) R13Q-TprA. (*F*) Voltages for 50% block, *Vh*, for TPrA. Data points and error bars in *A*, *B*, *D*, and *E* are means ± SEs for 3–8 different single Na channels at each voltage. R13E = 33 μM; R13Q = 8 μM; DEA = 25 mM; TPrA = 5 mM. Curves are the result of fitting of experimental data points with Boltzmann function: $1/(1+\exp(z\delta(V-Vh)/25.4)$. Values for fitting parameters are given in Table 1. Estimates of means ± SEs for fitting parameters are those provided by nonlinear fitting routine in Sigmaplot version 8.0.

μ-conotoxin mutants (R13Q and R13E) in the region of the DEA binding site. Here, we present an electrostatic model describing the distribution of potential inside the channel created by binding of the positively charged μ-conotoxin, consistent with the experimental data presented above.

Model geometry and initial parameters

The general geometric features of the model system used for potential calculations were based on the likely broad similarity between pores of K channels (17,18) and those of Na channels, as well as many experimental studies that put constraints on the specific structure of the selectivity filter and overall conducting pathway of Na channels (19). More extensive considerations of these issues are provided elsewhere (10,20). The model that we adopted is generally consistent with data on membrane thickness, selectivity filter length, NMR-structure of the toxin, and experimental data on the DEA binding site, which is located about halfway across the drop in applied potential across the membrane. The model is also consistent with experiments showing accessibility of the channel to intracellularly applied blockers. The model channel geometry is depicted in Fig. 5 *A*. The toxin molecule is represented by a charged dielectric sphere. The pore is divided into an extracellular vestibule (I), selectivity filter (II), cavity (III), and inner cylinder (IV). The individual dielectric constants, ε, and Debye lengths, $\lambda = 1/k$, as well as geometrical parameters, can be easily and separately changed in each region of the pore for the analysis of their effects on the potential attributable to toxin. Parameters chosen for the basic variant of the channel model (Table 2, case 1) were: $k_{\mathrm{I}} = 0$, $\varepsilon_{\mathrm{I}} = 80$, $r_{\mathrm{I}} = 14$ Å; $k_{\mathrm{II}} = 0$, $\varepsilon_{\mathrm{II}} = 10$, $r_{\mathrm{II}} = 1.5$ Å; $k_{\mathrm{III}} = 1/7$, $\varepsilon_{\mathrm{III}} = 80$, $r_{\mathrm{III}} = 6$ Å; and $k_{\mathrm{IV}} = 1/7$, $\varepsilon_{\mathrm{IV}} = 80$, $r_{\mathrm{IV}} = 3$ Å. In the surrounding solution and the body of the channel protein, parameters were, for region A, surrounding solution, $k = 1/7$, $\varepsilon = 80$; for region B, membrane/protein, $\varepsilon = 10$; and for region C/H, toxin, $\varepsilon = 10$, $r = 10$ Å. The distance between the center of the toxin sphere and the beginning of the channel was 3 Å.

TABLE 1 Parameters for fits of voltage-dependent block by DEA and TPrA

	ΔVh (mV)	$Vh \pm$ SE (mV)	Apparent valence $z\delta \pm$ SE
DEA			
Control (R13Q)		50 ± 1	0.53 ± 0.02
R13Q bound	23	73 ± 1	0.55 ± 0.01
Control (R13E)		54 ± 1	0.51 ± 0.01
R13E bound	16	70 ± 1	0.52 ± 0.01
TPrA			
Control (R13Q)		37 ± 2	0.57 ± 0.03
R13Q bound	9	46 ± 3	0.49 ± 0.04
Control (R13E)		36 ± 2	0.57 ± 0.05
R13E bound	7	43 ± 2	0.53 ± 0.03

Vh = voltage for 50% block; $z\delta$ is apparent valence. The shift, $\Delta Vh = \{Vh(\text{R13}x) - Vh(\text{control R13}x)\}$. DEA = 25 mM; TPrA = 5 mM. For other details, see legend of Fig. 3. Estimates of SEs of the means for fitting parameters are provided by nonlinear fitting routine of Sigmaplot version 8.0.

Electrostatic potential inside the channel, and distance between toxin and amine binding sites

The model assumes, for simplicity, that the binding of neither toxin nor DEA causes any conformational changes in the channel molecule, and that the location of the DEA binding site is the same in all cases, i.e., toxin-free, R13Q-bound, and

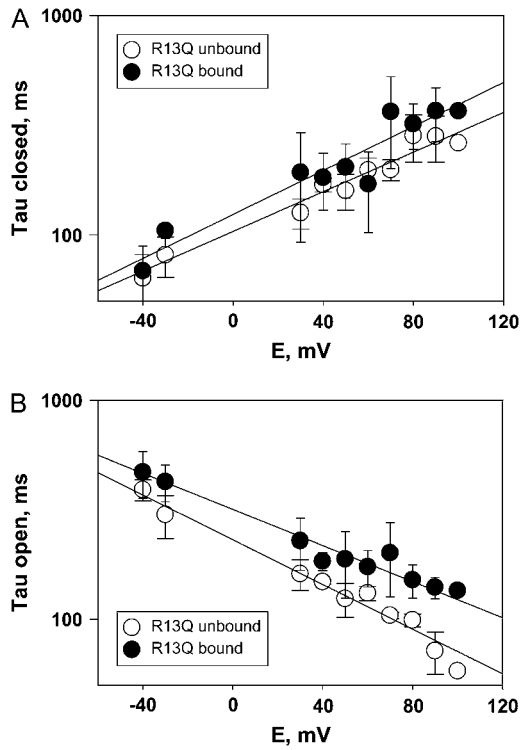

FIGURE 4 Voltage-dependence of open (unblocked) and blocked times for TPrA block. (*A*) Voltage-dependence of open times. (*B*) Voltage-dependence of blocked times. Estimates of mean open and blocked times were each obtained from dwell-time histograms with at least 100 events. Data presented are from three separate experiments. Error bars represent standard deviation.

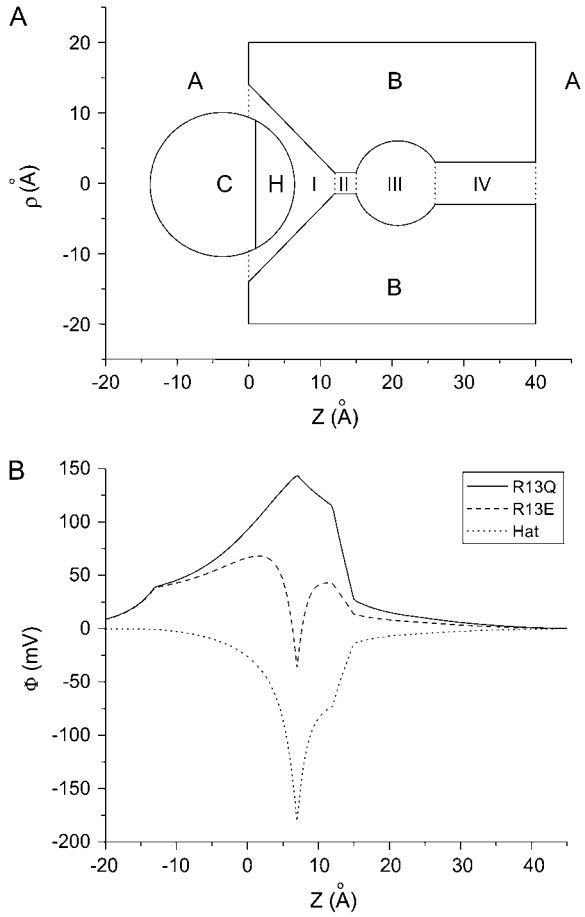

FIGURE 5 Modeling the electrostatic potential profile arising from toxin bound to channel's outer vestibule. (*A*) Geometry and physical parameters of model. The R13Q molecule is represented by a uniformly charged dielectric sphere; H denotes ''hat'' in which the extra negative of R13E is uniformly distributed. The pore is divided into an extracellular vestibule (area I), selectivity filter (area II), inner cavity (area III), and inner cylinder (area IV). For each region, the individual dielectric constants, ε, and Debye lengths, $\lambda = 1/k$, as well as geometrical parameters, can easily be changed for analysis of effects on toxin's contribution to the potential. Parameters chosen for the basic model were: $k_I = 0$, $\varepsilon_I = 80$, $r_I = 14$ Å; $k_{II} = 0$, $\varepsilon_{II} = 10$, $r_{II} = 1.5$ Å; $k_{III} = 1/7$, $\varepsilon_{III} = 80$, $r_{III} = 6$ Å; $k_{IV} = 1/7$, $\varepsilon_{IV} = 80$, $r_{IV} = 3$ Å. Region A: surrounding solution ($k = 1/7$, $\varepsilon = 80$). Region B: membrane ($\varepsilon = 10$). Region C: toxin ($\varepsilon = 10$, $r = 10$ Å). Distance between the center of sphere and the plane, outer surface of the channel was 3 Å. (*B*) Electrostatic potential contributions of R13Q (*solid curve*), R13E (*dashed curve*), and negative ''hat'' alone (*dotted curve*). R13Q (+5) was modeled as a uniformly charged sphere, and R13E (+4.5) was treated as a uniformly charged sphere, plus a hat with negative charge of −0.5e. The binding site location was defined as the position at which the calculated potential matched the appropriate experimentally measured shift.

R13E-bound channels. Electrostatic potential profiles were calculated for 14 different parameter sets, for each of three cases (Table 2). Although the final choice of this set was arbitrary, the set was designed to reveal possible sensitivity to our choices of key parameter values. First, R13Q was modeled as a uniformly charged sphere with a net charge of +5 evenly distributed over the sphere. Second, R13E was depicted with a negatively charged ''hat'' (*H* in Fig. 5 *A*) that

TABLE 2 Parameters used for DEA-toxin distance calculations presented in Fig. 5 *B*, where each distance calculated reflects one set of parameters

	I			III			IV		
	k_I (Å^{-1})	ε_I	r_I (Å)	k_{III} (Å^{-1})	ε_{III}	r_{III} (Å)	k_{IV} (Å^{-1})	ε_{IV}	Qhat (e)
1*	0	80	14	0.143	80	6	0.143	80	−0.5
2	0	80	14	0	80	5	0	80	−0.5
3	0	80	14	0	80	6	0	80	−0.5
4	0	40	14	0	80	6	0	40	−0.5
5	0.143	80	14	0	80	6	0	80	−0.5
6	0	80	14	0.143	80	5	0.143	80	−0.5
7	0	80	14	0.143	40	6	0.143	40	−0.5
8†	0	80	14	0.143	80	6	0.143	80	−0.5
9	0	80	14	0.143	80	6	0.143	80	−0.6
10	0	80	14	0.143	80	6	0.143	80	−1.0
11	0	80	14	0.143	40	6	0.143	40	−0.4
12	0	80	12	0.143	80	6	0.143	80	−0.5
13‡	0	80	12	0.143	80	6	0.143	80	−0.5
14	0	80	12	0.143	40	6	0.143	40	−0.5

Regions I, III, and IV correspond to the regions identified in Fig. 5 *A*. Qhat (e) is the charge on region H, defined in Fig 5 *A*; e is the elementary charge. For all 14 cases, parameters for selectivity filter (area II) are: $k_{II} = 0$, $\varepsilon_{II} = 10$.
*The base case.
†Dielectric constant of toxin is $\varepsilon = 20$ for this case. For other cases, $\varepsilon = 10$.
‡Length of selectivity filter is $L_{II} = 5$ Å for this case. For other cases, $L_{II} = 3$ Å.

carries the charge of the glutamate side chain, with the remaining +5 contribution to the charge distributed uniformly over the sphere. Third, to test whether the difference between R13Q-induced and R13E-induced shifts could be calculated directly, we used an uncharged sphere with a negatively charged hat (−0.5), *H*. In most calculations, the charge assigned to the 13-glutamate side chain, when R13E is bound to the channel, was −0.5, based on our earlier analysis of pH dependence (21). The effect of varying this charge on model predictions was also explored (Table 2, cases 9–11). Electrostatic potential profiles (Φ) calculated for these three cases for the basic variant of the model are shown in Fig. 5 *B*.

The position of the DEA binding site can be determined from the point where the calculated contribution of the toxin to the potential equals the experimentally determined potential shift of DEA block caused by toxin-binding, e.g., where $\Phi = (z\delta Vh)_{R13Q} - (z\delta Vh)_{unbound}$. These calculations give us three values for the distance for three differently charged spheres (two toxin derivatives, and the hat charge alone). This allows us to check the self-consistency of potential calculations, because values obtained for the distances should fulfill the following criteria. The distance estimates should be the same, within experimental error, and the DEA binding site should be located inside the water-filled cavity (region III, Fig. 5 *A*), consistent with both functional data and structural studies on K channels, and homology models of Na channels (22,23). As shown in Fig. 6, the basic case (*line 1*) fulfills these requirements, suggesting that the model provides a satisfactory estimation of electrostatic potential.

Next, we investigated the sensitivity of the model to changes in parameter values. To do so, we modified the initial parameters used in the base model, calculated the potential profiles for different toxins, and tested how well the distances obtained fulfilled the model requirements (Table 2, cases 2–14). The model was particularly sensitive to the value of *k*, proportional to the reciprocal of the Debye length. When *k* was set at 0 in areas III and IV, the estimated distance between binding sites was located in area IV (Fig. 6 *B*, and cases 2–5 in Table 2). This is not easy to reconcile with experimental data that suggest an amine binding site deep inside the cavity (area III), near the inner end of the selectivity filter. The model was also sensitive to the charge of the hat: change of the charge to −0.6e or −1e was associated with inconsistency in the distance calculation for different toxins (cases 9 and 10). In contrast, moderate changes of such parameters as dielectric constants in all areas, size of the areas, or *k* in area I did not lead to significant changes in distance calculations.

Evidence of coupling between binding of blockers and permeant ions within the channel

The simplified electrostatic model presented above treats the amine blockers as unit point charges that bind, and at the same physical location in the channel. The fact that TPrA exhibits a weaker interaction with the toxins than does DEA, in both the kinetic analysis shown in Fig. 9 of Ma et al. (7) and in the analysis of voltage-dependence of the amine block here (Fig. 3), suggests that additional factors must be considered in developing a full understanding of the toxin-amine interaction. The interaction may not be exclusively a direct electrostatic one, but may involve, instead or in addition, coupling between blocker binding and the probability of occupancy of different channel sites by permeating ions. Coupling between permeant ions and the binding of either amine or toxin was tested in two separate series of experiments.

In the first series of experiments, the effect of raising the external sodium concentration in the block by DEA was examined. At a constant voltage (+50 mV), this resulted in a significant decrease in the block by DEA (Fig. 7). This is illustrated in Fig. 7 *C* ($p = 0.02$), and might be intuitively explained in two ways. First, an increase in probability of occupancy by Na^+ of a site external to the amine-blocking site may provide a repulsive interaction with the blocking DEA. Second, there may be direct competition for the amine binding site by Na^+. In either case, the net result would be a coupling between the tendency for sodium to move into the external vestibule, and a decrease in the likelihood of block by internal DEA.

In a second series of experiments, we determined the relationship between unitary conductance in symmetric solutions and the concentration of sodium. Because of the slow toxin-binding kinetics, data were available for both toxin-bound and unbound channels from the same record. In the range of 10 mM to 1 M, the data are reasonably well-described by a simple rectangular hyperbola, as shown in Fig. 8 and in earlier studies (24,25). The estimated maximal single-channel conductance drops in the toxin-bound state, reflecting a partial

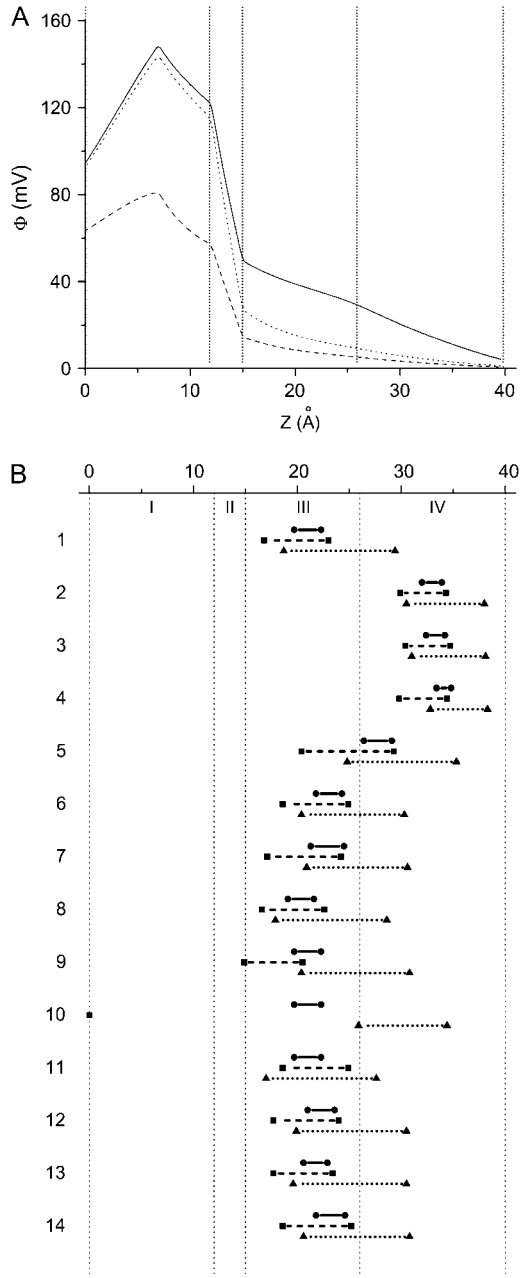

FIGURE 6 Sensitivity of model to parameter changes. (*A*) Electrostatic potential attributable to R13Q-molecule inside the channel for three cases of distribution of k inside the channel. The solid curve (case A): $k = 0$ in the whole channel. The dotted curve:: $k = 0$ in the vestibule and filter; $k = 1/7$ Å^{-1} in the cavity and inner cylinder. The dashed curve (case B): $k = 1/7$ Å^{-1} in the whole channel. For all cases, $k = 1/7$ Å^{-1} in the surrounding solution. Geometry of the system and spatial distribution of dielectric constant were as indicated in Fig. 3. Potential profiles for other cases of possible distribution of k inside the channel lie between curves for cases A and B (not shown). Plots show a steep drop of potential inside the filter, and also the effect of screening in the cavity and inner cylinder. (*B*) Estimated limits on binding-site position for DEA in 14 cases, for which the bound ''toxin'' was R13Q (*solid circles, solid connecting lines*), R13E (*solid squares, dashed connecting lines*), or the negative ''hat'' (*solid triangles, dotted connecting lines*). In the case of the negative ''hat,'' the position at which the calculated potential matched the difference between shifts induced by R13Q and R13E was used to define the binding-site location. Other parameters used for each of the 14 cases are shown in Table 2. The indicated range of values for each position estimate represents mean ± 1 SE, calculated from variances of experimentally measured parameters: the relevant half-blocking potentials and effective valences (see Fig. 3 and Table 2).

block of the channel, and notably, in the present context, the [Na^+] for half-maximal conductance increases ~4-fold for the R13Q-bound channel compared with the toxin-free channel (a change from ~7 to 31 mM; Fig. 8). Thus, when the toxin binds, there must be a change in probability of occupancy of the channel by sodium, and/or a redistribution of sodium occupancy among different energy minima in the conducting pathway. Thus, R13Q might affect amine block, at least in part, by changing the pattern or degree of sodium occupancy within the channel.

DISCUSSION

We investigated the voltage dependence of amine block of sodium channels partially blocked by two μ-conotoxin derivatives with different charges. Toxin binding causes a shift of amine block toward more positive voltages, consistent with an electrostatic trans-channel interaction between external and internal blockers. Using BEM, we calculated the electrostatic potential inside a simple, continuum model of a channel in the presence of μ-conotoxin, and showed that the observed shifts for DEA block are generally compatible with an electrostatic interaction. Small but systematic differences in behavior of two monovalent amines, DEA and TPrA, suggest that their depiction as point charges in the calculations may be a significant oversimplification. Additional data indicate significant coupling between permeant ions and binding of amines and toxin derivatives.

Interaction between amino blockers and permeant ions in voltage-gated channels

Amine blockers such as tetra-alkyl ammonium ions (TAA_{1-5}) are known to be internal blockers of voltage-gated sodium channels (5,26–28), as well as internal (29–31) and, in some cases, external (32) blockers of voltage-gated potassium channels.

Electrostatic repulsion is widely suggested to occur between conducting or blocking ions in K_V and Ca_V channels (32–35). An electrostatic interaction might also occur between the two blockers when they occupy sites in close proximity within the Na_V pore (6). However, Thompson and Begenisich (36) presented evidence against the idea that the mutual inhibition between tetra-ethyl ammonium (TEA) molecules binding to internal and external sites in K_V channels results primarily from direct, long-range electrostatic forces between TEA molecules. For example, TEA blocks *Shaker* from the outside in a voltage-dependent manner, but based on structural data, does not enter as deeply as suggested by the voltage-dependence (36). This was attributed to coupling be-

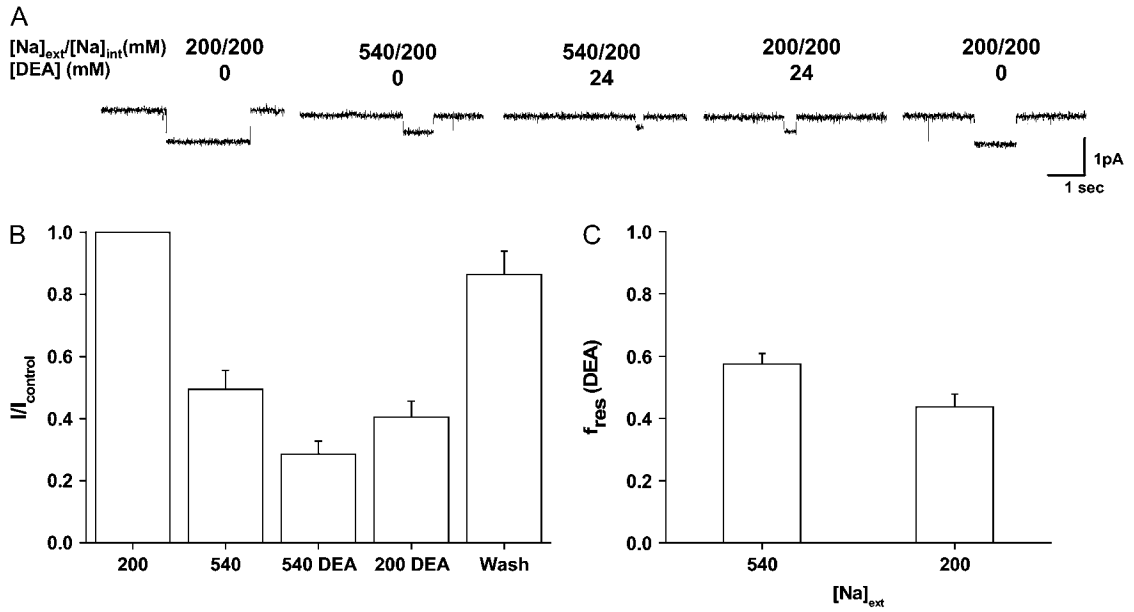

FIGURE 7 Increased external $[Na^+]$ decreases fractional block by internal DEA at a constant voltage. (*A*) Single-channel records at +50 mV show apparent unitary current amplitude throughout sequence of solution changes during an experiment. $[Na^+]_{ext}$ and $[DEA]_{int}$ were changed, as indicated, by perfusing the ''extracellular'' or ''intracellular'' chamber, respectively. (*B*) Summary data from four experiments show unitary current amplitudes, normalized relative to initial control values, as obtained in symmetric 200 mM Na^+, ± SE. The sequence of conditions was as shown in *A*. (*C*) Fractional residual current, f_{res} ± SE in the presence of 24 mM DEA, normalized to the amplitude under the same ionic conditions, but with 0 mM DEA. Block was reduced in the presence of higher external $[Na^+]$: $f_{res} = 0.58 \pm 0.07$ (540 mM; $f_{res} = 0.44 \pm 0.08$ (200 mM ext Na^+); $p = 0.02$ (paired *t*-test).

tween TEA binding and K^+ movement within the pore (37). A more negative voltage forces K^+ to move farther from the TEA binding site, thus increasing TEA binding affinity. By an extension of this argument, the location of permeant ions inside the pore is crucial for the trans-channel interaction between external and internal TEA applied to the *Shaker* potassium channel (38). In this case, externally bound TEA forces the K^+ ion to move deeper into the selectivity filter, where it causes stronger repulsion to the internally bound TEA than in the control case.

Antagonism between permeable ions and amino blockers was also shown for voltage-gated sodium channels (Figs. 7 and 8). Earlier studies showed that the replacement of external permeant sodium with impermeant N-methyl glucammonium increased the affinity of both rat skeletal muscle and bovine cardiac sodium channels for internal blockers, suggesting that sodium entering from the outside can repel internal amines (5,39). Conversely, a relief of block by internal tetra-pentyl ammonium was observed with increased external sodium in whole-cell patch-clamp experiments on cardiac sodium channels (28). Overall, these experiments suggest that the ions inside the pore can significantly affect blocker affinity, as measured under different conditions.

Nature of changes in amine block induced by μ-conotoxin binding

In our experiments, we evaluated the change of affinity of internally applied amine blockers associated with μ-conotoxin binding from the opposite side of the channel. Importantly, both of the μ-conotoxin derivatives used here blocked the single-channel current only partially, and there is no evidence that toxin-binding induces dramatic changes in pore geometry or channel selectivity (9). If partial occlusion of the pore caused by μ-conotoxin binding were to dramatically reduce the likelihood of Na^+ occupying the selectivity filter, one might expect an increase of amine-blocker affinity. In fact, as shown in Figs. 1–3, and in Ma et al. (7), amine block is reduced when one of the conotoxins binds. Thus, the mutual inhibition seen in our experiments might seem consistent with electrostatic repulsion between two blockers at their respective binding sites, rather than with redistribution of permeant ions among different sites inside the pore. This suggestion is further supported by our experiments insofar as the effect of the more positively charged R13Q (+5) μ-conotoxin on DEA binding was stronger than the effect of R13E (+4). These two μ-conotoxin derivatives differ only in the nature of the charged residue at position 13, and the relative block by an extended group of R13X derivatives is consistent with a conserved orientation of toxins within the channel (9).

Magnitudes of electrostatic and nonelectrostatic interactions of peptide ligands

In *Shaker* channels, the binding of singly charged TEA (+1) in the outer mouth of the channel causes a threefold decrease in the affinity of internally added TEA (+1) (38). This appears to result primarily from coupling to permeant ions within the channel, rather than by a direct electrostatic interaction between the two TEA ions. By contrast, in large-conductance Ca^{2+}-

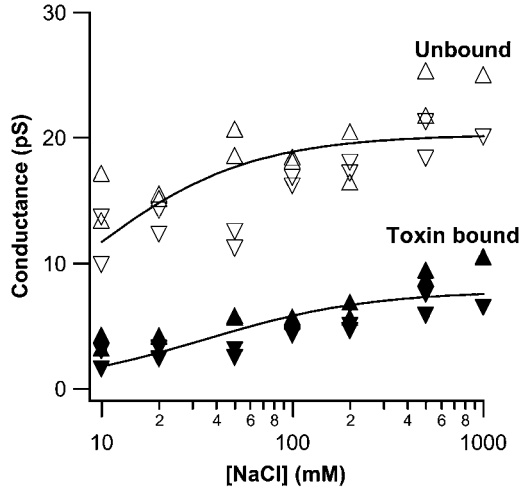

FIGURE 8 Binding of R13Q increases half-saturation concentration, $[Na^+]_{50}$, for unitary conductance amplitude in Na channels. The collected data are from 12 experiments, with data obtained at one or two concentrations in each experiment. Conductances were estimated at +40 mV (*upward triangles*) and −40 (*downward triangles*) in symmetric $[Na^+]$, and the parameters from the fits to the collected data were taken as estimates of values interpolated to 0 mV. Values for means ± SEs of parameters are those returned by Sigmaplot. Parameters were obtained from the fit of a Langmuir binding isotherm to each data set. Control (unbound): $[Na^+]_{50}$ = 7.0 ± 2.2 mM; R13Q bound: $[Na^+]_{50}$ = 31.4 ± 2.2 mM. Maximum conductances were control (unbound), 19.7 ± 1.3 pS; and R13Q bound, 7.4 ± 0.8 pS.

activated K^+ channels, the binding of highly charged dendrotoxin (DTX-I, +10), which partially occluded the channel from the inside, caused no statistically significant (~30% increase in Kd, $p = 0.1$) inhibition of the channel block by external TEA (40). For sodium channels, an apparently electrostatic interaction of R13Q (+5) with the strongly positive voltage sensor (net effective gating charge of approximately +12) shifted activation gating by only ~7 mV (6). This shift occurred instantaneously on R13Q binding to a single channel, and reversed immediately on dissociation. Together, these data indicate that electrostatic interactions between charged peptide and amine, or between peptide and voltage sensor, may be surprisingly weak, yet still reliably detectable. On the other hand, interactions among even monovalent ions, involving coupled redistribution among sites in a multiply occupied pore, can be quite strong. For our present data, the inhibitory interactions between toxin and amine, reflected in shifts of amine block by 7–23 mV, coincident with toxin binding (Table 1), are consistent with a contributing direct electrostatic interaction, but do not preclude additional effects of coupling to the redistribution of permeant ions within the pore, as suggested by data in Figs. 7 and 8.

Differing interactions of TPrA and DEA with toxins

Patch-clamp studies indicate that different tetra-alkylammonium (TAA_{1-5}) molecules bind approximately halfway along the potential drop across the channel, regardless of their size (28). This electrical distance to the binding site was estimated from the voltage-dependence of dissociation constants for a single-channel block. The large size differences among these molecules (maximal distance from *N* to the end of alkyl chain ranges from ~3.6 Å for tetra-methylammonium to ~8.8 Å for tetra-pentylammonium (28)) suggest that the side chains of larger amines may interact with the walls of the internal vestibule through hydrophobic interactions, whereas smaller amines probably reach their binding site directly through the water-filled pathway. The importance of hydrophobic interactions in the case of larger molecules can be seen from a comparison of their kinetics and affinity with such parameters of the smaller molecules. Our earlier work (5) showed that sodium-channel block by TEA is extremely fast (bound times, <0.1 ms), and that its affinity is relatively low (Kd ≈100 mM), whereas TPrA has a higher affinity (Kd ≈10 mM) and dramatically slower kinetics (blocked times, ~100 ms). Thus, the approach of a relatively small molecule like DEA to its binding site inside the channel might reasonably be modeled as a point charge passing through an aqueous environment. For larger, more hydrophobic molecules like TPrA, this simplification is more likely to break down. Recent molecular modeling suggests that even for the smaller tetra-methylammonium ion, Van der Waals interactions make a substantial contribution to stabilization in the sodium-channel outer vestibule (23).

Voltage-dependence of steady-state block

Attribution of a mechanism to the voltage-dependence of the apparent ''unidirectional'' rate constants (Fig. 4) is tricky. Voltage-dependence can depend on a number of factors, including ion interactions within the channel, and the relative likelihood of blocker exit by passing forward through the channel, or by dissociating back toward the side of origin. For example, the voltage-dependence of the block of a potassium channel by internal Na^+ was entirely associated with the binding rate constant, whereas dissociation was voltage-independent (41,42), suggesting that voltage-dependence arises from K^+ entry into the channel. A quite different scenario was reported for external divalent or trivalent ion blocks of calcium channels, where in most cases, the association was voltage-independent, and dissociation was accelerated by membrane hyperpolarization, which would favor exit in the forward (inward) direction (43).

In a broader context, several attempts were made to interpret the voltage-dependence of block, or electrical distance, in terms of the relative physical position of binding sites. In K channels, cytoplasmic blockers showed electrical distances from the cytoplasmic end that could be grouped systematically by size and chemical nature: tetra-alkylammonium ions, $n \geq 2 <$ Li, plus amines with polar side chains < Na, K, Cs, and Ba; see Table 2 in French and Shoukimas (44). Recent structural data confirm earlier suggestions (29,31) that tetra-alkylammonium blockers do not enter the narrow selectivity filter (45–47).

Furthermore, modeling indicates only a small voltage gradient in the inner cavity and cylinder of the pore, making it unlikely that the cytoplasmic amine blockers traverse a significant fraction of the transmembrane voltage (48). Thus, the voltage-dependence of these agents seems primarily to reflect a redistribution of permeant ions in the K-channel pore.

A similar argument might be applied to the voltage-dependence of local anesthetics and other amine blockers in sodium channels, even though, on average, it is likely that only a single Na^+ ion is present in the pore (25,49); but see Naranjo and Latorre (50). As with quaternary amine blockers in K channels, local anesthetics in Na channels appear to bind in the inner cavity, as reviewed and modeled by several groups (22,23,51,52). Here again, it is conceivable that the voltage-dependence of binding reflects, perhaps primarily but at least in part, a redistribution of Na^+ within the pore associated with local anesthetic binding.

In Na channels, despite general agreement that site 1 ligands, acting from the extracellular side, bind within the outer vestibule, the apparent electrical distances are similar for blockers with a range of sizes and net charges (tetrodotoxin and a variety of saxitoxin derivatives, net charges, -1 to $+2$) and μ-conotoxins (net charge, $+6$) (53,54). This ''common'' voltage-dependence may arise primarily from the shifting of Na^+ among sites, within the channel's voltage gradient, when the toxin binds, rather than crossing a substantial part of the transmembrane voltage by the toxin's own charge. This suggestion is also consistent with a more detailed study of conotoxin PIIIA derivatives, see McArthur and French (55) and the data in Fig. 8. Thus, it is plausible that, even in a ''single-occupancy'' Na channel, redistribution of the permeant ion may dominate the voltage-dependence of the block for such agents.

A simple model of trans-channel interactions resulting from direct electrostatic repulsion

Our continuum model gives self-consistent simulations of conotoxin-induced shifts in the voltage-dependence of block by DEA. The calculated location of the DEA binding site lies inside the inner water-filled cavity, close to the cytoplasmic end of the selectivity filter. Within experimental error, these calculated positions are similar for three different cases: R13Q, R13E, and an uncharged sphere with a negative point charge (-0.5) at the end. A value of -0.5 is the likely difference between charges the Q13 and E13 side chains of R13Q and R13E, bound in the pore under our experimental conditions, based on a functional analysis of the apparent pK (21). In the third case, the difference between shifts induced by R13Q and R13E was taken as the relevant experimental constraint. In most cases, the model was not very sensitive to variation of its parameters (Table 2 and Fig. 6). Ultimately, however, the model failed when tested against our observations with TPrA, because it did not account satisfactorily for the weaker interaction of TPrA with the conotoxins.

Influence of permeant ions on blocker binding and interactions

A direct indication that amine block is coupled to the gradient of permeant ions comes from the data in Fig. 7 *C*, showing a significant decrease in the fractional block by DEA when external [Na^+] was increased by 2.7-fold (fractional residual current, f_{res}, increased by $\sim$30%, from 0.58 to 0.44). This is intuitively explained as the result of an increased probability of occupancy by Na^+ of a site in the vicinity of the selectivity filter, on the extracellular side of the amine binding site.

Clearly, R13Q binding affects the apparent affinity of the channel for Na^+ (Fig. 8; R13Q binding induces a 4.5-fold increase in half-saturation concentration). However, the precise, expected influence of this coupling between the toxin and amines is hard to evaluate. For example, the fit in Fig. 8 suggests that, with symmetric 200 mM Na^+, the pore is likely to be singly occupied by Na^+ >95% of the time, even when R13Q is bound. This does not indicate exactly where, along the conducting pathway, the ion is most likely to reside, but the favored position would depend on the presence of bound toxin, and presumably would be biased by toxin-binding toward an energy minimum on the cytoplasmic side of the selectivity filter. For two synergistic reasons, R13Q binding would be expected to decrease the likelihood that a charged amine would bind in the inner cavity: 1), by a direct, electrostatic repulsion between the two positively charged ligands, and 2), by favoring occupancy by Na^+ of an energy minimum cytoplasmic to the selectivity filter, at or near the amine binding site. This view is consistent with homology model calculations of perturbations in electrostatic potential in the vicinity of bound conotoxins (9) and of lidocaine (22,23).

CONCLUSIONS

Tantalizingly, our data consistently imply a weaker interaction of each toxin with TPrA than with DEA; see Fig. 3 and Fig. 9 in Ma et al. (7). At first glance, this appears to be at odds with the observation that DEA and TPrA bind at the same electrical distance into the pore ($z\delta \approx 0.5$; Table 1). More than one factor may contribute to this apparent paradox. First, the modeling of amines as point charges may break down as the size is increased. Second, the mapping of electrical distance into physical space may not necessarily be identical for all toxin-amine combinations studied. Third, in sodium channels, the steep change in potential gradient is likely to be confined to an even shorter segment around the selectivity filter than in potassium channels (55,56). In the relatively wide inner cavity (segments III and IV in the model), the potential profile is likely to be relatively flat, making it difficult to detect small differences in physical position as changes in the electrical position of the binding site. Small differences in physical positions of charges for bound DEA and TPrA may be sufficient to affect interactions with nearby sodium ions, which secondarily modulate the overall toxin-amine

interaction. Nonetheless, calculations from a relatively simple electrostatic model reproduce, quite closely, the behavior from a complex set of experiments with DEA, R13Q, and R13E. Finally, an elegant examination of the role of cation-π electron interactions in the amine block of potassium channels by Ahern et al. (57) shows how critical the subtle details of chemical structure and orientation can be in determining the electrostatic component of a binding and blocking interaction. This point was underlined in their more recent study, which showed that cation-π interactions participate very specifically in the phasic, but not tonic, mode of block of cardiac sodium channels by lidocaine derivatives, and involve only one of three aromatic side chains present in the inner vestibule (58).

Our results show that, although voltage-gated Na channels do not show the dramatic consequences of multiple-ion occupancy that are common to many K and Ca channels, significant ion-ion interactions do occur within the Na-channel pore. Given that the partially blocking, R13X conotoxin derivatives allow ion conduction through the pore, this coupling must occur without obligatory trapping of even one permeant ion between a bound amine and the toxin. In contrast, the single-file selectivity filter of K channels, now confirmed by several high-resolution structures, clearly does allow ion-trapping.

In sodium channels, we suggest that the observed trans-channel interactions most likely arise from a combination of direct electrostatic interactions between toxin and amine blockers, with modulatory coupling to permeant ions in the pore. A full understanding of these interactions, and of the voltage-dependence of blocking reactions, will require an account of the transitions of permeant ions in and out of the steep part of the trans-channel potential gradient, and among different energy minima in the conducting pathway, as well as a knowledge of how the charge of the blocker itself moves in the electric field. Coupling between Na^+ ions and blockers occurs, although the weight of evidence suggests that, most of the time, the narrow part of the sodium channel accommodates only a single permeant ion. High-resolution Na channel structures will be invaluable in resolving the details of these issues.

Thanks go to Dr. Sergei Noskov for reading a draft of the manuscript. We are grateful to Dr. John Daly, NIDDK, for supplying us with batrachotoxin, to Christopher Bladen for making membrane preparations, and to Dr. Denis McMaster, Peptides Services, Faculty of Medicine, University of Calgary, for expert peptide synthesis and purification. We thank Drs. Dean McIntyre and Hans Vogel of the University of Calgary Bio-NMR Centre for NMR tests on the peptides.

This work was supported by the Canadian Institutes of Health Research, the Heart and Stroke Foundation of Alberta, NWT, and Nunavut, and the National Institutes of Health (Bethesda, MD). R.J.F. received salary support as a Medical Research Council/Canadian Institutes of Health Research Distinguished Scientist and as a Medical Scientist of the Alberta Heritage Foundation for Medical Research (AHFMR). G.W.Z. is an AHFMR Medical Scientist, and holds a Canada Research Chair. I.S. was supported by an AHFMR Studentship. Maintenance and operation of the Bio-NMR Centre is supported by the Canadian Institutes of Health Research and the University of Calgary.

REFERENCES

1. Woodhull, A. M. 1973. Ionic blockage of sodium channels in nerve. *J. Gen. Physiol.* 61:687–708.
2. Hille, B. 1975. Ionic selectivity of Na and K channels of nerve membranes. *In* Membranes—A Series of Advances. G. Eisenman, editor. Marcel Dekker, Inc., New York. 255–323.
3. French, R. J., and W. J. Adelman, Jr. 1976. Competition, saturation and inhibition—ionic interaction shown by membrane ionic currents in nerve, muscle and bilayer systems. *Curr. Topics Mem. Trans.* 8:161–207.
4. Strichartz, G. R. 1973. The inhibition of sodium currents in myelinated nerve by quaternary derivatives of lidocaine. *J. Gen. Physiol.* 62:37–57.
5. Zamponi, G. W., and R. J. French. 1994. Amine blockers of the cytoplasmic mouth of sodium channels: a small structural change can abolish voltage dependence. *Biophys. J.* 67:1015–1027.
6. French, R. J., E. Prusak-Sochaczewski, G. W. Zamponi, S. Becker, A. S. Kularatna, and R. Horn. 1996. Interactions between a pore-blocking peptide and the voltage sensor of the sodium channel: an electrostatic approach to channel geometry. *Neuron.* 16:407–413.
7. Ma, Q., E. Pavlov, T. Britvina, G. W. Zamponi, and R. J. French. 2008. Trans-channel interactions in batrachotoxin-modified rat skeletal muscle sodium channels. Kinetic analysis of mutual inhibition between μ-conotoxin GIIIA derivatives and amine blockers. *Biophys. J.* 4266–4276.
8. Chang, N. S., R. J. French, G. M. Lipkind, H. A. Fozzard, and S. Dudley, Jr. 1998. Predominant interactions between μ-conotoxin Arg-13 and the skeletal muscle Na^+ channel localized by mutant cycle analysis. *Biochemistry.* 37:4407–4419.
9. Hui, K., G. Lipkind, H. A. Fozzard, and R. J. French. 2002. Electrostatic and steric contributions to block of the skeletal muscle sodium channel by μ-conotoxin. *J. Gen. Physiol.* 119:45–54.
10. Tikhonov, D. B., and B. S. Zhorov. 2005. Modeling p-loops domain of sodium channel: homology with potassium channels and interaction with ligands. *Biophys. J.* 88:184–197.
11. Choudhary, G., M. P. Aliste, D. P. Tieleman, R. J. French, and S. C. Dudley, Jr. 2007. Docking orientation of μ-conotoxin GIIIA in the sodium channel outer vestibule. *Channels.* 1:344–352.
12. Paris, F., and J. Canas. 1997. Boundary Element Method. Fundamentals and Applications. Oxford University Press, Oxford.
13. Yoon, B. J., and A. M. Lenhoff. 1992. Computation of the electrostatic interaction energy between a protein and a charged surface. *J. Phys. Chem.* 96:3130–3134.
14. Juffer, A. H., P. Argos, and H. J. Vogel. 1997. Calculating acid-dissociation constants of proteins using the boundary element method. *J. Phys. Chem. B.* 101:7664–7673.
15. Hoyles, M., S. Kuyucak, and S.-H. Chung. 1996. Energy barrier presented to ions by the vestibule of the biological membrane channel. *Biophys. J.* 70:1628–1642.
16. Chung, S. H., T. W. Allen, and S. Kuyucak. 2002. Conducting-state properties of the KcsA potassium channel from molecular and Brownian dynamics simulations. *Biophys. J.* 82:628–645.
17. Doyle, D. A., J. M. Cabral, R. A. Pfuetzner, A. Kuo, J. M. Gulbis, S. L. Cohen, B. T. Chait, and R. MacKinnon. 1998. The structure of the potassium channel: molecular basis of K^+ conduction and selectivity. *Science.* 280:69–77.
18. Long, S. B., E. B. Campbell, and R. MacKinnon. 2005. Crystal structure of a mammalian voltage-dependent *Shaker* family K^+ channel. *Science.* 309:897–903.
19. Hille, B. 2001. Ion Channels of Excitable Membranes. Sinauer Associates, Inc., Sunderland, MA.
20. Lipkind, G. M., and H. A. Fozzard. 2000. KcsA crystal structure as framework for a molecular model for the Na^+ channel pore. *Biochem.* 39:8161–8170.
21. Hui, K., D. McIntyre, and R. J. French. 2003. Conotoxins as sensors of local pH and electrostatic potential in the outer vestibule of the sodium channel. *J. Gen. Physiol.* 122:63–79.

22. Lipkind, G. M., and H. A. Fozzard. 2005. Molecular modeling of local anesthetic drug binding by voltage-gated sodium channels. *Mol. Pharmacol.* 68:1611–1622.

23. Tikhonov, D. B., and B. S. Zhorov. 2007. Sodium channels: ionic model of slow inactivation and state-dependent drug binding. *Biophys. J.* 93:1557–1570.

24. Moczydlowski, E., S. S. Garber, and C. Miller. 1984. Batrachotoxin-activated sodium channels in planar lipid bilayers: competition of tetrodotoxin block by Na^+. *J. Gen. Physiol.* 84:665–686.

25. French, R. J., J. F. Worley III, W. F. Wonderlin, A. S. Kularatna, and B. K. Krueger. 1994. Ion permeation, divalent ion block and chemical modifications of single sodium channels: description by single-occupancy, rate theory models. *J. Gen. Physiol.* 103:447–470.

26. French, R. J., and R. Horn. 1983. Sodium channel gating: models, mimics and modifiers. *Annu. Rev. Biophys. Bioeng.* 12:319–356.

27. O'Leary, M. E., and R. Horn. 1994. Internal block by human heart sodium channels by symmetrical tetra-alkylammoniums. *J. Gen. Physiol.* 104:507–522.

28. O'Leary, M. E., R. G. Kallen, and R. Horn. 1994. Evidence for a direct interaction between internal tetra- alkylammonium cations and the inactivation gate of cardiac sodium channels. *J. Gen. Physiol.* 104:523–539.

29. Armstrong, C. M. 1966. Time course of TEA^+-induced anomalous rectification in squid giant axons. *J. Gen. Physiol.* 50:491–503.

30. Armstrong, C. M., and B. Hille. 1972. The inner quaternary ammonium ion receptor in potassium channels of the node of Ranvier. *J. Gen. Physiol.* 59:388–400.

31. French, R. J., and J. J. Shoukimas. 1981. Blockage of squid axon potassium conductance by internal tetra-*n*-alkylammonium ions of various sizes. *Biophys. J.* 34:271–291.

32. Newland, C. F., J. P. Adelman, B. L. Tempel, and W. Almers. 1992. Repulsion between tetraethylammonium ions in cloned voltage-gated potassium channels. *Neuron.* 8:975–982.

33. Bernèche, S., and B. Roux. 2001. Energetics of ion conduction through the K^+ channel. *Nature.* 414:73–77.

34. Almers, W., E. W. McCleskey, and P. T. Palade. 1984. A non-selective cation conductance in frog muscle blocked by micromolar external calcium ions. *J. Physiol.* 353:565–583.

35. Hess, P., and R. W. Tsien. 1984. Mechanism of ion permeation through calcium channels. *Nature.* 309:453–456.

36. Thompson, J., and T. Begenisich. 2003. External TEA block of *Shaker* K^+ channels is coupled to the movement of K+ ions within the selectivity filter. *J. Gen. Physiol.* 122:239–246.

37. Thompson, J., and T. Begenisich. 2005. Two stable, conducting conformations of the selectivity filter in *Shaker* K^+ channels. *J. Gen. Physiol.* 125:619–629.

38. Thompson, J., and T. Begenisich. 2000. Interaction between quaternary ammonium ions in the pore of potassium channels. Evidence against an electrostatic repulsion mechanism. *J. Gen. Physiol.* 115:769–782.

39. Zamponi, G. W., and R. J. French. 1993. Dissecting lidocaine action: diethylamine and phenol mimic separate modes of lidocaine block of sodium channels from heart and skeletal muscle. *Biophys. J.* 65:2335–2347.

40. Favre, I., and E. Moczydlowski. 1999. Simultaneous binding of basic peptides at intracellular sites on a large conductance Ca^{2+}-activated K^+ channel. Equilibrium and kinetic basis of negatively coupled ligand interactions. *J. Gen. Physiol.* 113:295–320.

41. Yellen, G. 1984. Ion permeation and blockade in Ca^{2+}-activated K^+ channels of bovine chromaffin cells. *J. Gen. Physiol.* 84:157–186.

42. Yellen, G. 1984. Relief of Na^+ block of Ca^{2+}-activated K^+ channels by external cations. *J. Gen. Physiol.* 84:187–199.

43. Lansman, J. B., P. Hess, and R. W. Tsien. 1986. Blockade of current through single calcium channels by Cd^{2+}, Mg^{2+} and Ca^{2+}. Voltage and concentration dependence of calcium entry into the pore. *J. Gen. Physiol.* 88:321–347.

44. French, R. J., and J. J. Shoukimas. 1985. An ion's view of the potassium channel. The structure of the permeation pathway as sensed by a variety of blocking ions. *J. Gen. Physiol.* 85:669–698.

45. Zhou, M., J. H. Morais-Cabral, S. Mann, and R. MacKinnon. 2001. Potassium channel receptor site for the inactivation gate and quaternary amine inhibitors. *Nature.* 411:657–661.

46. Faraldo-Gomez, J. D., E. Kutluay, V. Jogini, Y. Zhao, L. Heginbotham, and B. Roux. 2007. Mechanism of intracellular block of the KcsA K^+ channel by tetrabutylammonium: insights from x-ray crystallography, electrophysiology and replica-exchange molecular dynamics simulations. *J. Mol. Biol.* 365:649–662.

47. Yohannan, S., Y. Hu, and Y. Zhou. 2007. Crystallographic study of the tetrabutylammonium block to the KcsA K^+ channel. *J. Mol. Biol.* 366:806–814.

48. Jogini, V., and B. Roux. 2005. Electrostatics of the intracellular vestibule of K^+ channels. *J. Mol. Biol.* 354:272–288.

49. Ravindran, A., H. Kwiecinski, O. Alvarez, G. Eisenman, and E. Moczydlowski. 1992. Modeling ion permeation through batrachotoxin-modified Na^+ channels from rat skeletal muscle with a multi-ion pore. *Biophys. J.* 61:494–508.

50. Naranjo, D., and R. Latorre. 1993. Ion conduction in substates of the batrachotoxin-modified Na^+ channel from toad skeletal muscle. *Biophys. J.* 64:1038–1050.

51. Tikhonov, D. B., I. Bruhova, and B. S. Zhorov. 2006. Atomic determinants of state-dependent block of sodium channels by charged local anesthetics and benzocaine. *FEBS Lett.* 580:6027–6032.

52. Scheib, H., I. McLay, N. Guex, J. J. Clare, F. E. Blaney, T. J. Dale, S. N. Tate, and G. M. Robertson. 2006. Modeling the pore structure of voltage-gated sodium channels in closed, open, and fast-inactivated conformation reveals details of site 1 toxin and local anesthetic binding. *J. Mol. Model.* 12:813–822.

53. Moczydlowski, E., S. Hall, S. S. Garber, G. R. Strichartz, and C. Miller. 1984. Voltage dependent blockade of muscle Na^+ channels by guanidinium toxins: effect of toxin charge. *J. Gen. Physiol.* 84:687–704.

54. Becker, S., E. Prusak-Sochaczewski, G. Zamponi, A. G. Beck-Sickinger, R. D. Gordon, and R. J. French. 1992. Action of derivatives of μ-conotoxin GIIIA on sodium channels. Single amino acid substitutions in the toxin separately affect association and dissociation rates. *Biochemistry.* 31:8229–8238.

55. McArthur, J. R., and R. J. French. 2007. An attempt to determine the orientation of μ-conotoxin binding to sodium channels by mapping the contributions of individual residues to the voltage dependence of block. *Biophys. J.* 92(Suppl.):178a.

56. McNulty, M. M., G. B. Edgerton, R. D. Shah, D. A. Hanck, H. A. Fozzard, and G. M. Lipkind. 2007. Charge at the lidocaine binding site residue Phe-1759 affects permeation in human cardiac voltage-gated sodium channels. *J. Physiol. Lond.* 581:741–755.

57. Ahern, C. A., A. L. Eastwood, H. A. Lester, D. A. Dougherty, and R. Horn. 2006. A cation-pi interaction between extracellular TEA and an aromatic residue in potassium channels. *J. Gen. Physiol.* 128:649–657.

58. Ahern, C. A., A. L. Eastwood, D. A. Dougherty, and R. Horn. 2008. Electrostatic contributions of aromatic residues in the local anesthetic receptor of voltage-gated sodium channels. *Circ. Res.* 102:86–94.